JOURNAL OF THE KOREAN ASTRONOMICAL SOCIETY
37: 237 ~ 241, 2004

THE VELOCITY FIELD OF SUPERNOVA-DRIVEN TURBULENCE IN THE INTERSTELLAR MEDIUM

JONGSOO KIM
Korea Astronomy Observatory, 61-1, Hwaam-Dong, Yusong-Ku, Taejon 305-348, Korea
E-mail: jskim@kao.re.kr
(Received July 30, 2004; Accepted December 10, 2004)

ABSTRACT

We perform numerical experiments on supernova-driven turbulent flows in order to see whether or not supernovae play a major role in driving turbulence in the interstellar medium. In a $(200\mathrm{pc})^3$ computational box, we set up, as initial conditions, uniformly magnetized gas distributions with different pairs of hydrogen number densities and magnetic field strengths, which cover the observed values in the Galactic midplane. We then explode supernovae at randomly chosen positions at a Galactic explosion rate and follow up the evolution of the supernova-driven turbulent flows by integrating numerically the ideal MHD equations with cooling and heating terms. From the numerical experiments we find that the density-weighted velocity dispersions of the flows are in the range of 5-10 km s^{-1}, which are consistent with the observed velocity dispersions of cold and warm neutral media. Additionally, we find that strong compressible flows driven by supernova explosions quickly change into solenoidal flows.

Key words : methods:numerical — MHD —turbulence

I. INTRODUCTION

It is a well-known fact that the line widths of molecular species in molecular clouds are supersonic if their linear sizes are larger than 0.05 pc (e.g., Larson 1981). It is also true that the column-density weighted velocity dispersions of HI 21 cm lines of cold and warm neutral media are mildly supersonic (e.g., Heiles & Troland 2003). So the large portion of the line widths of, at least, molecular and neutral gas in the interstellar medium are due to turbulent motions of gas. However, the origin of the turbulent motions is not known, yet.

One idea proposed by Arons & Max (1975) is that the turbulent motions are due to Alfvénic waves, because i) a typical Alfvén velocity is larger than a sound speed in the interstellar medium, ii) linear Alfvén waves with small amplitudes hardly decay. Recent numerical experiments done by Stone et al. (1998), Mac Low et al. (1998), Padoan et al. (1998), however, showed that supersonic compressible magnetohydrodynamic turbulence, which includes Alfvén waves, decays in the order of the flow crossing time. This short decay time of the turbulence brings a new idea that turbulence should be continuously driven by some mechanisms. Several possible driving mechanisms, such as a) cloud-cloud collisions, b) expansion of HII regions, c) stellar winds, d) galactic shear, and e) spiral arms and hydraulic jumps, have been put forward so far, and they were reviewed by Mac Low & Klessen (2004) and Elmegreen & Scalo (2004). Of the several candidates, the energy input rate from supernova explosions is the largest one (Mac Low & Klessen 2004). In this work, by measuring velocity dispersions of supernova-driven turbulent flows directly through numerical experiments, we show that supernovae play a major role in driving turbulence in the interstellar medium.

II. NUMERICAL METHOD AND PARAMETERS

We solve the ideal MHD equations in a conservative form with cooling and heating processes:

$$\frac{\partial \rho}{\partial t} + \nabla \cdot (\rho \mathbf{v}) = 0, \tag{1}$$

$$\frac{\partial}{\partial t}(\rho \mathbf{v}) + \nabla \cdot \left[\rho \mathbf{v}\mathbf{v} + \left(p + \frac{B^2}{8\pi}\right)\mathbf{I} - \frac{\mathbf{B}\mathbf{B}}{4\pi}\right] = 0, \tag{2}$$

$$\frac{\partial \mathbf{B}}{\partial t} + \nabla \cdot (\mathbf{v}\mathbf{B} - \mathbf{B}\mathbf{v}) = 0, \tag{3}$$

and

$$\frac{\partial E}{\partial t} + \nabla \cdot \left[\left(E + p + \frac{\mathbf{B}^2}{8\pi}\right)\mathbf{v} - (\mathbf{v}\cdot\mathbf{B})\frac{\mathbf{B}}{4\pi}\right] = \Gamma - \Lambda, \tag{4}$$

where $\mathbf{I}$ is the unitary tensor, the total energy E is defined by $p/(\gamma - 1) + \rho\mathbf{v}^2/2 + \mathbf{B}^2/(8\pi)$, Γ and Λ are heating and cooling rate per volume, and other notations follow their usual conventions. The numerical calculations were done using the RIEMANN framework, which is based on higher-order Godunov schemes for MHD (Balsara 1998a,b). The framework is highly suited for astrophysical flows by incorporating schemes for pressure positivity (Balsara and Spicer 1999a), and divergence-free magnetic field (Balsara and Spicer 1999b; Balsara & Kim 2004).

Proceedings of The 2nd Korea-Mexico Joint Workshop on *Physics of the Diffuse Interstellar Medium*

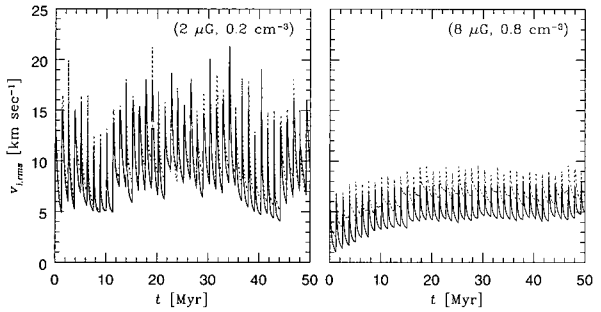

Fig. 1.— Density-averaged velocity dispersions for two models with 2 μG and 0.2 cm^{-3} (left panel), and 8 μG and 0.8 cm^{-3} (right panel). Solid and dotted lines represent dispersions along the mean field (x-) direction and the other (y-) direction, respectively.

The volumetric cooling rate Λ is dependent upon $n_e n_H L(T)$, where n_e and n_H are the electron and hydrogen (including ionized one) number densities, and $L(T)$ is a cooling curve. We use a tabulated version of the radiative cooling curve shown in Figure 1 of MacDonald and Bailey (1981), which is based on the works of Raymond, Cox & Smith (1976) and Shapiro and Moore (1976). In order to prevent the gas from cooling below zero, we set a lower temperature cutoff at 100 K. We also include a heating term Γ, which is proportional to the hydrogen number density. We set a heating level such that the initial equilibrium temperature T_{eq} determined by a heating and cooling balance is 8000 K.

A typical supernova explosion rate including both type I and II is 0.014 per year in the Galaxy (Cappellaro et al. 1999). If we take the effective volume of the Galaxy for supernova explosions to be $\pi \times (15\text{kpc})^2 \times 0.2\text{kpc}$, then the time interval between two consecutive supernova explosions in our computational box becomes 1.26 Myr. We exploded supernovae one at a time at a randomly chosen position in our computational box. For simplicity, we don't take into account of clustered supernova explosions. Each supernova explosion dumps 10^{51} erg thermal energy into a sphere with a radius 5 pc.

We assume an ideal gas with a ratio of specific heats $\gamma = 5/3$. Its temperature is determined from the equation of state $p = \rho kT/\mu$, where k is Boltzman's constant and μ is the mean molecular weight. We assume a constant $\mu = (14/23)m_H$, which corresponds to a complete ionized gas with a 10% number ratio of helium to hydrogen. Simulations have been carried out in a (200 pc)^3 computational box, which is covered with 256^3 cells. A periodic condition is used for whole boundaries. We run 9 models with different combinations of three values for density $(0.2, 0.4, 0.8) \times 1.4 m_H$ cm^{-3} and three values for field strength, 2μG, 4μG, and 8μG. The initial field direction is aligned with the x-axis.

III. VELOCITY DISPERSION

It is the velocity dispersion that enables us to see whether supernovae become a possible candidate for turbulence in the interstellar medium. We measure density-weighted velocity dispersions as a function of time for each model. From 9 models, we find that the levels of the dispersions are dependent upon total (gas+magnetic) pressure. Dispersions are small (large) in high (low) total environmental pressure. This is because the size of a supernova remnant becomes smaller as the total pressure increases, and so does the high-velocity region swept by the remnant.

We select two extreme models: one with 2 μG, 0.2 cm^{-3} gives the lower end of the total pressure in our models, and the other with 8 μG, 0.8 cm^{-3} does the upper end, both of which bounds the velocity dispersions in our models. We plot the density-averaged velocity dispersions for both models in Figure 1. The model parameters are indicated in each panel. Solid lines represent velocity dispersions along the mean field direction for the two cases. Because of the similarity of dispersions along two directions perpendicular to the mean field x-direction, we plot only the dispersions of the y component with dotted lines. Each supernova explosion event makes one spike in the plot. The jump of the velocity dispersions shown in the environment with the low total pressure (left panel) is higher than that with the high total pressure (right panel). The velocity dispersions of the latter case are saturated at certain levels, while those of the former case are quite fluctuating. In order to give typical values of the velocity dispersions, we take time averages over the whole time interval for the left panel and the interval after 15 Myr for the right panel. The averaged x- and y-component values 9.1 km sec^{-1} and 9.9 km sec^{-1}, respectively, for the left panel, and they are 5.1 km sec^{-1} and 7.1 km sec^{-1} for the right panel.

IV. VELOCITY SPECTRA

In our models, a turbulent flow is generated by a physically motivated driving source, supernova. It is quite different in some ways from, an idealized driving source, a Gaussian random distribution in Fourier space with a predefined functional form, which has been used in most turbulence simulations. A supernova explosion releases an enormous amount of energy at a point. As an outwardly propagating shock wave sweeps the ambient medium, the size of a supernova remnant keeps increasing. When an expansion velocity of the remnant becomes similar to the root-mean-square velocity of the ambient medium, the size gets saturated. So one characteristic of the supernova driving is that, even the supernova energy is put at the tiny scale, the peak wavelength of energy power spectra keeps increasing up to a typical size of the supernova remnant. Another characteristic is that, by the nature of the blast wave, the supernova explosion initially generates a strong com-

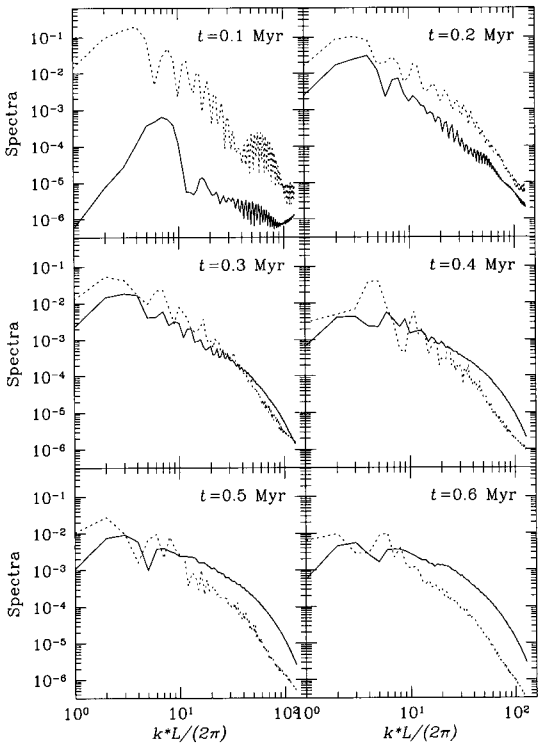

Fig. 2.— Velocity power spectra of a flow generated by a single supernova explosion. In each frame solid and dotted lines represent power spectra of solenoidal and compressible components, respectively. Please note that a time epoch in each frame is the same as the one at the corresponding frames in Figures 3 and 4.

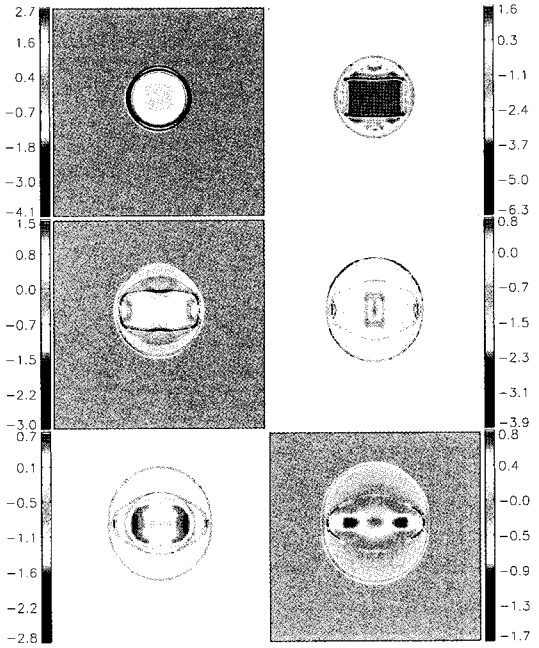

Fig. 3.— Color-coded images of $\nabla \cdot \vec{v}$ at six time epochs. The image plane passes through an explosion center and its horizontal axis is aligned with the mean field direction. Time epochs from a top-left frame to a bottom-right one are 0.1, 0.2, 0.3, 0.4, 0.5, 0.6 Myr, respectively.

pressible flow. Because of these characteristics, it is quite interesting to see spectral properties of the turbulence driven by supernova explosions.

In order to see time evolution of spectral properties of the flow generated by a single supernova event, we show in Figure 2 time-series spectra of solenoidal and compressible components of velocity fields. The hydrogen number density and field strength of the initial ambient medium are 0.8 cm^{-3} and 8 μG, respectively. If we look at the upper-left frame, which is a snapshot at the earliest time epoch of frames in Figure 2, the compressible component (a dotted line) has far more power than the solenoidal one (a solid line). This is an expected result, because an outwardly propagating shock wave generates a compressible flow. As time goes one, the solenoidal spectra, however, gradually catch up during the time interval $t = 0.2 - 0.3$ Myr, and even have more power than the compressible ones later, especially at wavenumbers larger than $kL/(2\pi) = 10$. This is an interesting observation, because the initially strong compressible flow could easily be converted into the solenoidal one. It is, however, not clear to us how such conversion occurs. It seems that the conversion mainly occurs at shocked regions where the levels of $|\nabla \times \vec{v}|$ are higher than other regions (see Fig. 4).

To visualize compressible and solenoidal components of the velocity fields in real space, we plot divergence and curl of the velocity fields on a (x, y) plane which passes through an explosion center as color-coded images in Figure 3 and Figure 4, respectively. Please note that the time epoch of each frame in Figure 3 and Figure 4 is the same as that of the frame at the corresponding location in Figure 2. The outermost expanding wave with larger negative values of $\nabla \cdot \vec{v}$, which actually delineates the outer shape of the supernova remnant, is well resolved in Figure 3. Up to about 0.1 Myr that is the end epoch of the energy-conserving phase, the remnant has a spherical shape. Afterwards, its shape becomes elongated along the vertical direction of the images. (Please note that the initial magnetic field direction is aligned with the horizontal axis of the images.) This elongation is due to the fact that the magnetosonic wave with a fastest wave speed propagates along the vertical direction. Because of the compressive nature of the magnetosonic wave, its propagation could be also seen in the images of divergence $\vec{v}$. In fact, the two blue-colored horizontal lines seen in the upper-right panel of Figure 3 represent a snapshot of the vertical propagation of the wave. In the upper-right panel of Figure 4, there is no clear signature of the magnetosonic wave. However, we can easily find in Figure 4 that the strong solenoidal flows generate in shocked regions.

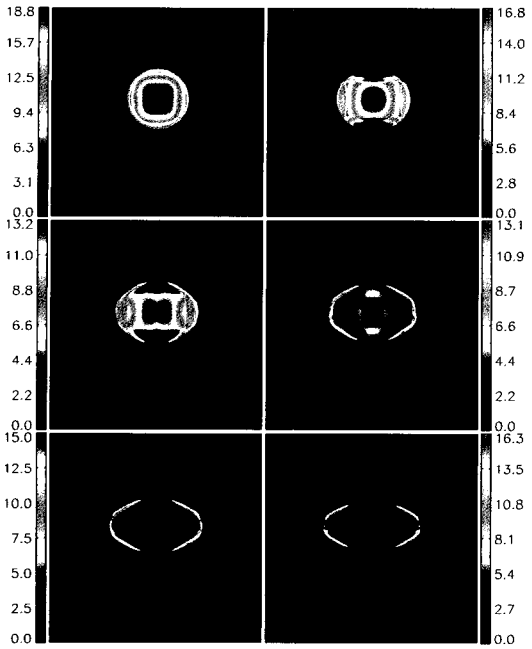

Fig. 4.— Color-coded images of $|\nabla \times \vec{v}|$ at six time epochs. The image plane passes through an explosion center and its horizontal axis is aligned with the mean field direction. Time epochs from a top-left frame to a bottom-right one are 0.1, 0.2, 0.3, 0.4, 0.5, 0.6 Myr, respectively.

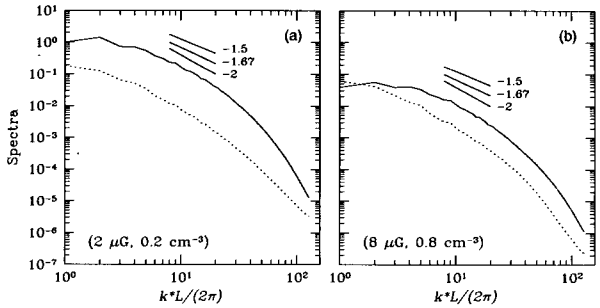

Fig. 5.— Time-averaged velocity power spectra of solenoidal and compressible components. The solid and dotted lines represent the solenoidal and compressible components, respectively. Each spectrum in the left panel (a) is obtained by averaging over 10 time epochs from 5 Myr to 50 Myr with a 5 Myr interval from a simulation with an initial magnetic field strength and a hydrogen density being (2 μG, 0.2 cm^{-3}). The right panel (b), however, averaged over 7 epochs from 20 Myr to 50 Myr with parameters (8 μG, 0.8 cm^{-3}).

Figure 5 shows time-averaged power spectra of solenoidal and compressible components of velocity fields from two of our models. The left panel (a) is averaged over 10 time epochs from 5 Myr to 50 Myr with a 5 Myr interval from a simulation with initial model parameters, a magnetic field strength and a hydrogen density, being (2 μG, 0.2 cm^{-3}). The left panel (b) is however averaged over 7 time epochs from 20 to 50 Myr with the same interval from a simulation with parameters (8 μG, 0.8 cm^{-3}). The reason why we exclude the early evolutionary stage in the average for the right panel is that the velocity dispersions during the early stage shown in Figure 2 are lower than the later converged level. In each panel we include three straight line segments with slopes -1.5, -5/3, and -2 for the spectra of Iroshinikov (1964) and Kraichnan (1965), Kolmogorov (1941), and Burgers (1974) turbulences, respectively. Due to the limited numerical resolution and the numerical dissipation, the inertial ranges of the spectra are quite small. The wavenumber ranges covered by the line segments might be within the initial ranges. The comparison of the slopes of the spectra with those of three line segments enables us to read a slope of our spectra, which is around -2. In fact, this is an expected slope of the spectra of shock-dominated turbulence, which, in our case, is generated by supernova explosions.

From the above numerical experiment of the single supernova explosion in a uniformly magnetized medium, we know that the initially strong compressible flow generated by the explosion could be easily converted to the solenoidal one. For the cases with multiple supernova explosions at randomly chosen positions, the hot interiors of different supernova remnants merge each other and naturally form a "tunnel network" (Cox & Smith 1974). In such an inhomogeneous environment, significant portion of the strong compressible outward flow by a new explosion can be changed into the solenoidal flow by the interaction with nearby dense clumps (obstacles). In fact, Figure 5, the time-averaged velocity power spectra in such an inhomogeneous environments, shows that the solenoidal component dominates the compressible one. Additionally, we can find in Figure 5 that the levels of spectra in the left panel are higher than those in the right panel, which is due to the effect of the difference of total environment pressures. Similar behavior in real space was also seen in Figure 1.

V. CONCLUSION AND DISCUSSIONS

The prime purpose of this work is to show that supernovae can become a major driving source for the interstellar turbulence. We indeed showed through the numerical simulations that the velocity dispersions are in the range of 5 - 10 km s^{-1}, which are consistent with the column-density weighted velocity dispersions of cold and warm HI clouds (Heiles & Troland 2003).

Supernova explosions from massive stars are correlated, and form superbubbles. This has a strong impact in the volume affected by each explosion, and in the final amount of energy available for turbulent motions (see for instance Franco et al. 1991; Ferriere 1998). We didn't however take into account the superbubbles in this current work. Inclusion of them into the current

numerical setup will become the next topic of our research.

Also, the plasma ejected from SN explosions is not always in a smooth density distribution. It seems to come out in a fragmented way, due to instabilities generated in the initial acceleration phase. The resulting fragments interact in a different way that the rest of the ejecta, and will stir the shocked material, adding vorticity and cooling at the early phases of remnant evolution (see Franco et al. 1993), which may be poorly resolved in our computations due to the limited numerical resolution. However, we are quite sure that the measured velocity dispersion of the whole computational box, a global quantity, is not sensitive to numerical resolution.

ACKNOWLEDGEMENTS

I am grateful to J. Franco for providing me comments, and my collaborators, M.-M. Mac Low, and D. Balsara for their contributions to this work.

REFERENCES

Arons, J., & Max, C. E. 1975, ApJ, 196, L77

Balsara, D. S. 1998a, ApJS, 116, 119

Balsara, D. S. 1998b, ApJS, 116, 133

Balsara, D. S., & Kim, J. 2004, ApJ, 602, 1079

Balsara, D. S., & Spicer D. 1999a, J. of Comput. Phys., 148, 133

Balsara, D. S., & Spicer D. 1999b, J. of Comput. Phys., 149, 270

Burgers, M. M. 1974, The Nonlinear Diffusion Equation (Dordrecht: Reidel)

Cappellaro, E., Evans, R., & Turatto, M. 1999, A&A, 351, 459

Cox, D. P., & Smith B. W. 1974, ApJ, 189, 105

Elmegreen, B. G., & Scalo, J. 2004, ARA&A, submitted (astro-ph/0404451)

Ferriere, K. 1998, ApJ, 503, 700

Franco, J, Tenorio-Tagle, G., Tenorio-Tagle, G., & Bodenheimer, P. 1991, PASP, 103, 137

Franco, J, Ferrara, A., Rozyczka, M., Tenorio-Tagle, G., & Cox, D. P. 1993, ApJ, 407, 100

Heiles, C., & Troland, T. H. 2003, ApJS, 145, 329

Iroshinikov, P. 1964, Soviet Astron., 7, 566

Kolmogorov, A. 1941, Dokl. Akad. Nauk SSR, 31, 538

Kraichnan, R. 1965, Phys. Fluids, 8 1385

Larson, R. B. 1981, MNRAS, 194, 809

MacDonald, J., & Bailey, M. E. 1981, MNRAS, 197, 995

Mac Low, M.-M., Klessen, R. S., Burkert, A., Smith, M. D., & Kessel, O. 1998, Phys. Rev. Lett, 80, 2754

Mac Low, M.-M., & Klessen, R. S. 2004, Rev. of Mod. Phys., 76, 125

Padoan, P, & Nordlund, A. 1999, ApJ, 526, 279

Raymond, J. C., Cox, D. P., & Smith, B. W. 1976, ApJ, 204, 290

Shapiro, P. R., & Moore, R. T. 1976, ApJ, 207, 413

Stone, J. M., Ostriker, E. C., & Gammie, C. F. 1998, ApJ, L99